

Activation Energy of Shear Transformation Zones: A Key for Understanding Rheology of Glasses and Liquids

S. G. Mayr*

I. Physikalisches Institut, Georg-August-Universität Göttingen, Friedrich-Hund-Platz 1, 37077 Göttingen, Germany
(Received 6 July 2006; published 6 November 2006)

Key manifestations of the glassy and liquid states, such as viscous flow and structural relaxation, occur spatial and temporal heterogeneously, within highly localized rare events, termed shear transformation zones. Characterization of these basic entities with respect to thermal activation and mechanical response is vital for understanding the rheology of glasses across length scales. This is achieved in classical molecular dynamics computer simulations on the model glass, CuTi, by determining the activation energy barrier and plastic yield strain of individual shear transformation zones as a function of size and external stress loading. Sizes of ≈ 140 atoms are identified to be especially energetically favorable with an activation energy barrier of ≈ 0.35 eV. Using these parameters, a rheology model is proposed to quantitatively explain viscosity.

DOI: 10.1103/PhysRevLett.97.195501

PACS numbers: 61.43.Fs, 62.10.+s, 83.50.-v

Identification of physical processes, which are responsible for dynamics and rheology in liquids and glasses, has attracted interest of numerous researchers during the past century. While first kinetic theories for viscous flow in liquids were based on the presumption of homogeneous flow [1] at vanishing shear modulus [2] in similarity to gases, it was first Frenkel [3] to point out analogies to solids, viz., a nonvanishing shear modulus [4] at comparable atomic packing densities. Both aspects have recently attracted renewed scientific interest due to the discovery of a highly heterogeneous dynamics on temporal and spatial time scales in melts and glasses [5,6]. Despite this rather long history and extensive experimental and theoretical efforts undertaken during the past two decades (see, e.g., [7–10] and references therein), the physics of melts and glasses is generally considered one of the great unresolved problems of condensed matter physics [11,12]. The main reason for this surely lies in the lack of structural order and the large number of nonreducible degrees of freedom involved, when compared to the crystalline counterparts. However, recent progress in experimental [13] and computational [14] methods have contributed to improve understanding.

Significant conceptual improvements to relate structure and energetics resulted from employing the concepts of potential energy landscapes (PEL) [15] to glasses and liquids by Debenedetti and Stillinger [16], viz., by considering the potential energy as a function of a generalized configurational parameter space. This allows for a natural interpretation of many materials properties, such as fragility [17] or relaxational dynamics, as will be discussed in more detail below. To explain plastic deformation, Johnson and Samwer [18] recently merged this picture with Argon's concept of shear transformation zones (STZs) [19], which recently received much promotion due to the works of Falk and Langer [20–22] and others [23,24]: in the zero temperature limit, shearing of a macroscopic glassy solid is basically interpreted as being composed of individual

highly localized shear events, which are activated, once the stress level within individual STZs reaches its corresponding yielding stress. However, a quantitative description remained unclear.

Inspired by these previous works, the present investigation aims to give a *quantitative* model for thermally activated anelasticity and plastic flow in glasses and liquids, respectively, at sufficiently low temperatures at moderate stresses, viz., in the absence of shear bands. We base our work on the assumption that the energetics within an individual STZ under applied shear stress can be described by a PEL, as schematically depicted in Fig. 1: before an STZ is thermally activated, its generalized configurational coordinates reside within the left local minimum, performing thermal vibrations, as well as configurational changes within the β relaxational dynamics. Flipping of an STZ to the second major local minimum occurs, once the corresponding soft vibrational mode receives enough thermal energy, E_A^* , to be activated. Clearly, E_A^* is reduced, as the

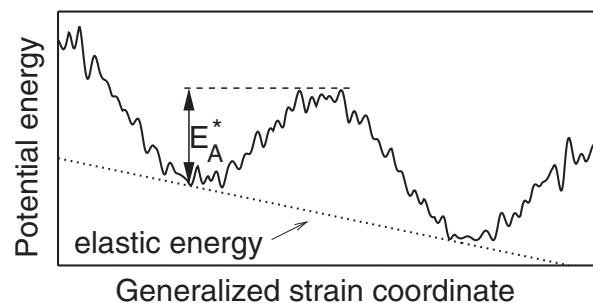


FIG. 1. Schematic illustration of the potential energy landscape of an individual STZ under applied shear stress: while activation of plastic shear events (α relaxation) requires energies of E_A^* , additional processes (β relaxation) which are not capable of significant shear deformation occur within the STZs. External shear stress tilts the potential energy landscape.

stress level on the STZ (i.e., slope of the elastic energy contribution in Fig. 1) increases.

Classical molecular dynamics (MD) simulations were performed on the model glass, $\text{Cu}_{50}\text{Ti}_{50}$, using a highly realistic embedded atom method (EAM) [25] interatomic potential, as parametrized by Sabochnik and Lam [26]. To enable a correct description of excited states, the short range pair interaction parts of the potential were splined to the Ziegler-Littmark-Biersack universal potential [27] for distances smaller than $\approx 1.6 \text{ \AA}$, as described before [28]. Amorphous cells, composed of 4500 atoms total [29], were prepared by quenching from melt (6000 K) with rates of 0.1 K/psec at zero pressure and periodic boundaries down to 10 K, using velocity and box rescaling algorithms of the Berendsen type [31] with time constants, $\tau_T = 300 \text{ fsec}$ and $\tau_P = 100 \text{ fsec}$, respectively. During quenching, both volume and enthalpy of the cell clearly showed the signatures of the glass transition, which occurred at $\approx 610 \text{ K}$. Amorphicity is additionally verified by evaluating the pair and angular distribution functions, respectively, which indicate the absence of long-range translational and orientational order. Successive heating and quenching cycles fail to further reduce the cell energy, which indicates a highly relaxed amorphous configuration of the cell. This is additionally corroborated by monitoring the usual time dependence of the atomic mean square displacements [32].

To investigate plastic strains as a result of excitation-induced shear events, the cell is in the following loaded with a constant biaxial compressive stress, σ , in the x and y directions, while zero stress is maintained in the z direction. A Berendsen-type of pressure control [31] with a large enough time constant, $\tau_P = 100 \text{ fsec}$, prevents the occurrence of artificial oscillatory responses—in particular, during the lifetime of an excitation. Plastic deformations are characterized by changes of the cell shape, viz., the plastic strain in z direction, ϵ_{zz} , which additionally has been corrected for possible changes in cell volume due to configurational changes within the amorphous CuTi. Excitations are introduced into the system by exposing all atoms within a radius R of an arbitrary chosen central point, $\vec{r} = (x, y, z)$ [a region, which we call “excited region (ER)” in the following] to Gaussian white noise of a predefined energy, E_E , while the rest of the atoms are thermostated towards 10 K using, again, a Berendsen [31] temperature control with $\tau_T = 300 \text{ fsec}$. This is achieved either (i) by assigning Gaussian random velocities of energy E_E to these atoms, or (ii) by randomly displacing these atoms according to a Gaussian distribution. In the latter case, the standard deviation of the displacements, ξ , were chosen to correspond to a potential energy of E_E according to the high temperature limit of a local Debye-Waller-like treatment [33], $\langle \xi^2 \rangle \approx \frac{3\hbar^2 E_E}{mk_B^2 \Theta^2}$, where $\Theta = 384 \text{ K}$ [34], m , and k_B denote the effective Debye temperature, the atom mass, and the Boltzmann constant, respectively. Both cases, (i) and (ii), result in

excitation of those vibrational modes of the system, which—at least partially—overlap with the ER. This way, only highly localized modes, which are located completely within the ERs [which we call “internal modes” (IM) in the following], end up with the specified energy, E_E , at the beginning of the excitations. All other modes [“external modes (EM)”], which exceed the ER regions due to their size or location, become less excited and transfer energy from the ER to the thermostated regions of the surrounding matrix. The lifetimes of ER, τ , as defined by a e^{-1} decay of their energy, are found to scale inversely with the surface to volume ratio of the ER, viz. $\tau \propto R$, with $\tau(R = 4 \text{ \AA}) \approx 67 \text{ fsec}$ and $\tau(R = 12 \text{ \AA}) \approx 130 \text{ fsec}$ (Fig. 2). This picture is additionally corroborated by the good agreement of τ with the vibrational period, τ_O , of external and internal modes, which we found to be approximately 110 fsec. As long as τ_T is chosen significantly larger ($\tau_T \gtrsim 200 \text{ fsec}$) than τ (or, equivalently, τ_O) these results prove to be greatly independent of the choice of τ_T in the thermostated regions of the cell, which show an energy dissipation with a time constant of $\approx 2\tau_T$, as expected (Fig. 2).

The above considerations make clear that this scenario is perfectly suited to determine the activation energies for viscous flow, E_A^* , and the corresponding plastic strains as a function of the spatial dimensions of the underlying soft modes—starting from either (i) purely kinetic or (ii) purely potential energy activations. This is performed for differently sized ER, ranging from $R = 4 \text{ \AA}$ to $R = 12 \text{ \AA}$, by monitoring the onset of plastic response during

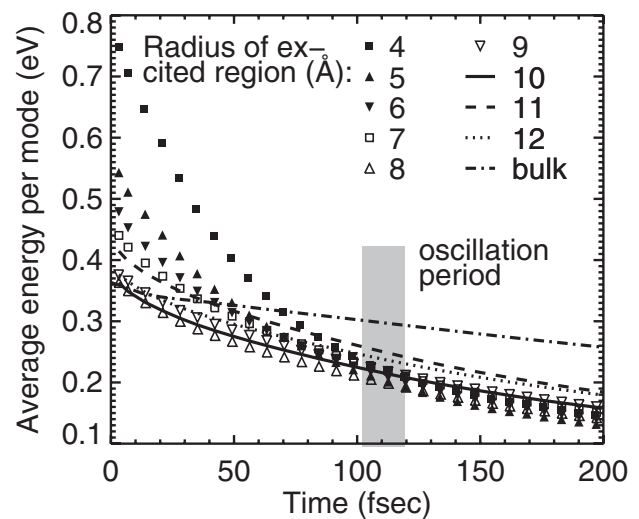


FIG. 2. Temporal evolution of the average energy per vibrational mode within spherical regions of specified radii, after exposition to sufficiently energetic Gaussian velocity excitations to overcome the activation barriers of at least one soft mode: the local energies dissipate with time constants, $\tau \lesssim 106 \text{ fsec}$, which are comparable to the period of oscillations within these regions, while the time constant imposed on the bulk cell by the temperature control (600 fsec) remains significantly larger.

series of 6000 or more excitations upon increase of E_E . Figure 3 shows a representative example, where Gaussian velocity excitations with $R = 8 \text{ \AA}$ are introduced into the system. While significant plastic relaxations start occurring at excitation energies as low as $\approx 0.322 \text{ eV}$, steady-state flow requires excitation energies, E_A , of at least 0.362 eV . As shown in Fig. 4, E_A shows a dramatic drop from $\approx 0.7 \text{ eV}$ down to $\approx 0.35 \text{ eV}$ when increasing the radius from 4 \AA to 8 \AA ; hereafter it reaches a steady value. Generally, E_A proves to be greatly independent of the type of excitations, relaxation state, thermodynamic ensemble (constant pressure or constant volume, respectively), and sign of the applied biaxial stress [35], which indicates its independence of the simulation details, and emphasizes its very fundamental relevance.

The considerations above and Fig. 4 clearly imply that soft modes with a spatial dimension of $R \approx 8 \text{ \AA}$ (or, equivalently, ≈ 140 atoms) [36] need a minimum activation energy of $\approx 0.35 \text{ eV}$ per mode for plastically flipping; here E_A^* equals E_A . Slightly elevated excitation energies, E_E , which exceed E_A^* , are merely capable of activating the same soft modes, and thus lead to approximately identical slopes in Fig. 3. Smaller ERs either lead to flipping of soft modes within the ER, which require elevated activation energies, or to activation of soft modes, which exceed the ERs. In both cases, higher values of E_A are necessary. Larger ER, on the other hand, lead to the activation of multiple identical soft modes, which all require the mini-

um activation energy of E_A^* , thus resulting in a constant value of $E_A = E_A^*$ in Fig. 4 in this regime. This latter statement is particularly corroborated by considering the slopes right at the onset of plastic flow, $\kappa = \frac{d\epsilon_{zz}}{dN}$, for differently sized ERs, as determined from plots similar to Fig. 3: κ is found to scale approximately linearly with the volume of the ER, $\frac{4\pi}{3}R^3$, for $R \geq 8 \text{ \AA}$ [e.g., $\kappa(R = 8 \text{ \AA}) = 2.42 \times 10^{-6}$ and $\kappa(R = 12 \text{ \AA}) = 7.77 \times 10^{-6}$ for Gaussian velocity excitations]. In this context it is necessary to point out that the activation energy of the most unstable soft modes strongly decreases as a function of stress—one example is given in the inset of Fig. 4.

We proceed further by discussing the consequences of our characterization of the minimum energy soft mode within a simple rheological model for the flow of glasses in the low-temperature limit, viz., typically around the glass transition temperature. Assuming that the PEL is only weakly temperature dependent, we first note that this most unstable mode will clearly be preferentially activated by thermal fluctuations, and thus regard it—for simplicity—as the only unstable mode present in the system. Furthermore, it is assumed that the temperature is low enough, that different STZs are independently activated, while they particularly do not overlap. Using, again, the biaxial geometry, the viscosity is then given by:

$$\eta = \frac{\sigma}{3\dot{\epsilon}_{zz}}. \quad (1)$$

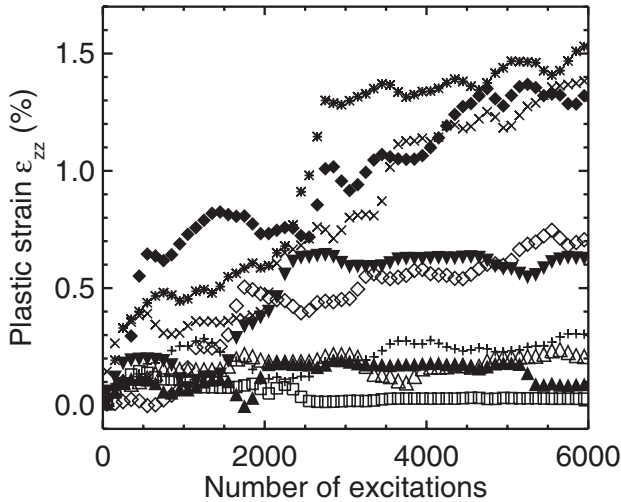


FIG. 3. Plastic deformations, ϵ_{zz} , in amorphous CuTi at 10 K base temperature due to Gaussian velocity excitations in random spherical regions of a fixed radius, $R = 8 \text{ \AA}$ (139 atoms), at variable excitation energies, E_E (selection of representative data with $E_E = \triangle: 0.271 \text{ eV}$, $\square: 0.284 \text{ eV}$, $\blacktriangle: 0.297 \text{ eV}$, $+: 0.309 \text{ eV}$, $\blacktriangledown: 0.322 \text{ eV}$, $\diamond: 0.348 \text{ eV}$, $\times: 0.362 \text{ eV}$, $*: 0.375 \text{ eV}$, $\blacklozenge: 0.388 \text{ eV}$). While plastic relaxations start occurring at energies as low as $\approx 0.322 \text{ eV}$, the activation energy of viscous flow (ϵ_{zz} becomes a linear function of number of excitations) is $\approx 0.362 \text{ eV}$.

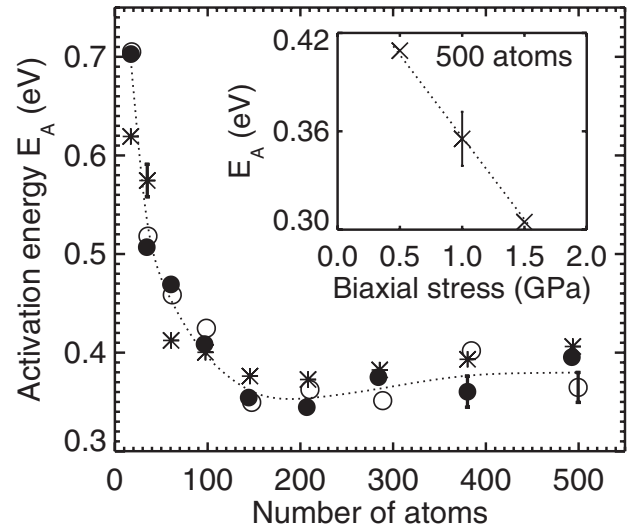


FIG. 4. Activation energies, E_A , for viscous flow due to successive shear events within spherical regions of variable sizes (main plot): for each size, E_A is determined during an energy series of 6000 Gaussian displacement (●) and velocity (○) excitations each (as shown in Fig. 3). The asterisk symbols (*) correspond to Gaussian displacement excitations, which were performed in an unrelaxed cell under constant volume conditions. The inset shows—as an example—the decrease of the activation energies as a function of stress.

While $\sigma = 0.5$ GPa is constant throughout all runs, $\dot{\epsilon}_{zz}$ is determined in the following way for thermal activation: $\kappa_0 := \kappa(R = 8 \text{ \AA}) \approx 2.041 \times 10^{-6}$ measures the average strain per soft mode, multiplied by the number of soft modes per $n_A = 4500$ atoms. In the thermal case, for each available soft mode in the system, such an activation attempt occurs every half oscillation period with a probability given by the Boltzmann factor, viz., with a rate of $\frac{2}{\tau_O} e^{-(E_A^*/k_B T)}$, where $E_A^* = 0.352$ eV and a typical value for $\tau_O = 110$ fsec are assumed. Thus, the total strain rate is given by:

$$\dot{\epsilon}_{zz} = n_A \kappa_0 \frac{2}{\tau_O} e^{-(E_A^*/k_B T)} = 3.12 \times 10^8 \frac{1}{\text{fsec}}. \quad (2)$$

To countercheck the validity of our model, we compare the predicted viscosity, η_P , with the corresponding ‘‘experimental’’ value, η_E , which we obtained by monitoring the steady-state thermal flow of our cell at 650 K, while biaxial stresses in the x and y directions were applied:

$$\eta_P = 0.534 \text{ Pa} \cdot \text{sec} \quad \text{and} \quad \eta_E = 0.565 \text{ Pa} \cdot \text{sec}. \quad (3)$$

Both values are in excellent agreement, which confirms our model assumptions and interpretations.

To conclude, we have quantitatively determined key parameters of thermally activated STZs in the model glass, CuTi, viz., the size, activation energies, and plastic yield. Cast in a thermodynamic model, this parameter triple can quantitatively explain thermally activated viscous flow and creep at moderate temperatures. It is straightforward to generalize these results to other STZ dominated phenomena, such as aging or crystallization.

The author acknowledges Professor Dr. K. Samwer, Georg-August-Universität Göttingen, Germany, and Professor Dr. W.L. Johnson, California Institute of Technology, Pasadena, CA, USA, for valuable discussions and support. Part of the computations were performed at the Gesellschaft für wissenschaftliche Datenverarbeitung, Göttingen (GWDG), Germany. Financial support by the DFG, SFB 602, TP B3, is gratefully acknowledged.

*Electronic address: smayr@gwdg.de

- [1] S. Glasstone, K.J. Laidler, and H. Eyring, *The Theory of Rate Processes* (McGraw-Hill, New York, 1941).
- [2] M. Born, *J. Chem. Phys.* **7**, 591 (1939).
- [3] I. A. Frenkel, *Kinetic Theory of Liquids* (Clarendon, Oxford, 1946).
- [4] A. S. Bains, C. A. Gorgon, A. V. Granato, and R. B. Schwarz, *J. Alloys Compd.* **310**, 20 (2000).
- [5] H. Sillescu, *J. Non-Cryst. Solids* **243**, 81 (1999).
- [6] S. G. Mayr, *J. Appl. Phys.* **97**, 096103 (2005).
- [7] J. Zarzycki, *Glasses and the Vitreous State* (Cambridge University Press, Cambridge, England, 1982).
- [8] S. R. Elliott, *Physics of Amorphous Materials* (Longman Scientific, London, 1990).
- [9] P. G. Debenedetti, *Metastable Liquids: Concepts and Principles* (Princeton University Press, Princeton, NJ, 1996).
- [10] Excellent reviews on models and experiments can be found in *J. Non-Cryst. Solids*. Vol. 307–310 (2002).
- [11] P. W. Andersen, *Science* **267**, 1615 (1995).
- [12] M. D. Ediger, C. A. Angell, and S. R. Nagel, *J. Phys. Chem.* **100**, 13200 (1996).
- [13] P. Lunkenheimer, U. Schneider, R. Brandl, and A. Loidl, *Contemp. Phys.* **41**, 15 (2000).
- [14] K. Binder and W. Kob, *Glassy Materials and Disordered Solids* (World Scientific, Singapore, 2005).
- [15] D. J. Wales, *Energy Landscapes* (Cambridge University Press, Cambridge, England, 2003).
- [16] P. G. Debenedetti and F. H. Stillinger, *Nature (London)* **410**, 259 (2001).
- [17] C. A. Angell, *J. Non-Cryst. Solids* **102**, 205 (1988).
- [18] W. L. Johnson and K. Samwer, *Phys. Rev. Lett.* **95**, 195501 (2005).
- [19] A. S. Argon, *Acta Metall.* **27**, 47 (1979).
- [20] M. L. Falk and J. S. Langer, *Phys. Rev. E* **57**, 7192 (1998).
- [21] M. L. Falk and J. S. Langer, *MRS Bull.* **25**, 40 (2000).
- [22] J. S. Langer, *Scr. Mater.* **54**, 375 (2006).
- [23] C. A. Schuh and A. C. Lund, *Nat. Mater.* **2**, 449 (2003).
- [24] H. D. Stevenson, J. Schmalian, and P. G. Wolynes, *Nature Phys.* **2**, 268 (2006).
- [25] M. S. Daw and M. I. Baskes, *Phys. Rev. B* **29**, 6443 (1984).
- [26] M. J. Sabochick and N. Q. Lam, *Phys. Rev. B* **43**, 5243 (1991).
- [27] J. F. Ziegler, J. P. Biersack, and U. Littmark, *The Stopping and Range of Ions in Matter* (Pergamon, New York, 1985).
- [28] S. G. Mayr, *Phys. Rev. B* **71**, 144109 (2005).
- [29] As the STZ size is expected to be ≈ 120 atoms [18,30], a cell of 4500 atoms proves to be large enough to correctly cover all relevant physics of STZs: test calculations with 3.5×10^4 atoms lead to consistent results.
- [30] M. Zink, K. Samwer, W. L. Johnson, and S. G. Mayr, *Phys. Rev. B* **73**, 172203 (2006).
- [31] H. J. C. Berendsen, J. P. M. Postma, W. F. van Gunsteren, A. DiNola, and J. R. Haak, *J. Chem. Phys.* **81**, 3684 (1984).
- [32] C. Oligschleger and H. R. Schober, *Phys. Rev. B* **59**, 811 (1999).
- [33] C. Kittel, *Quantum Theory of Solids* (Wiley, New York, 1963).
- [34] Θ was used as a fitting parameter to obtain the desired excitation energy, E_E .
- [35] This suggests a vanishing activation volume for viscous flow. Uniaxial stress or pure shear stress leads to consistent results.
- [36] It is interesting to note that this spatial dimension agrees reasonably well with the correlation length of the plastic displacement field during forced deformation below T_g [30].